

Stress Relaxation After Steady Shearing: Applications and Empirical Representation*

EMORY MENEFEE, *Western Regional Research Laboratory, Western Utilization Research and Development Division, Agricultural Research Service, U. S. Department of Agriculture, Albany, California*

Synopsis

The measurement of stress relaxation following steady-state shearing is particularly useful in the terminal relaxation zone, where the rheological properties are molecular weight dependent. This paper contains a description of the method as applied to molten polymers, and an empirical function found to be useful for fitting the data. Three examples are given to demonstrate some direct and simple applications. First, the decrease of viscosity with increasing shear rate may be estimated by simply replotting the experimental data. Second, extrapolation of calculated viscosities to very high shear rates is shown to lead to a possible explanation for melt fracture. Third, the true Newtonian viscosity can be estimated from measurements conducted at a nonzero shear rate.

Introduction

In studying the rheological properties of soft materials such as polymer melts, one has available a wide choice of experimental methods. These have been well summarized by Ferry.¹ The use of several techniques on the same material is usually redundant, although occasionally necessary to cover a broad time scale. There is, naturally, a diversity in the methods according to equipment requirements, time needed to make a measurement, and simplicity of calculations leading to a desired result.

It is intended in this paper to show how one such method, namely that of stress relaxation following steady-state shearing, can be used to reveal considerable useful information with relatively little effort. The general approach is aimed toward practical applications, but it is often true that approximate treatments can also provide insight into the detailed molecular processes, as will be illustrated by the example of melt fracture.

Discussion of the Method

The measurement of relaxation following steady flow is particularly useful in the terminal relaxation zone, where the rheological properties are molecular weight-dependent. The method was proposed some time ago

* Presented at West Coast Regional Meeting of the Society of Rheology at Pasadena, California, February 2, 1962.

by Schremp, Ferry, and Evans² but has for some reason found little subsequent use, and that mainly by Watkins.^{3,4} In the terminal region the method has, for most needs, several advantages over the more frequently used procedure of measuring stress relaxation following the sudden application of a strain. First, the steady-flow method weights the relaxation dis-

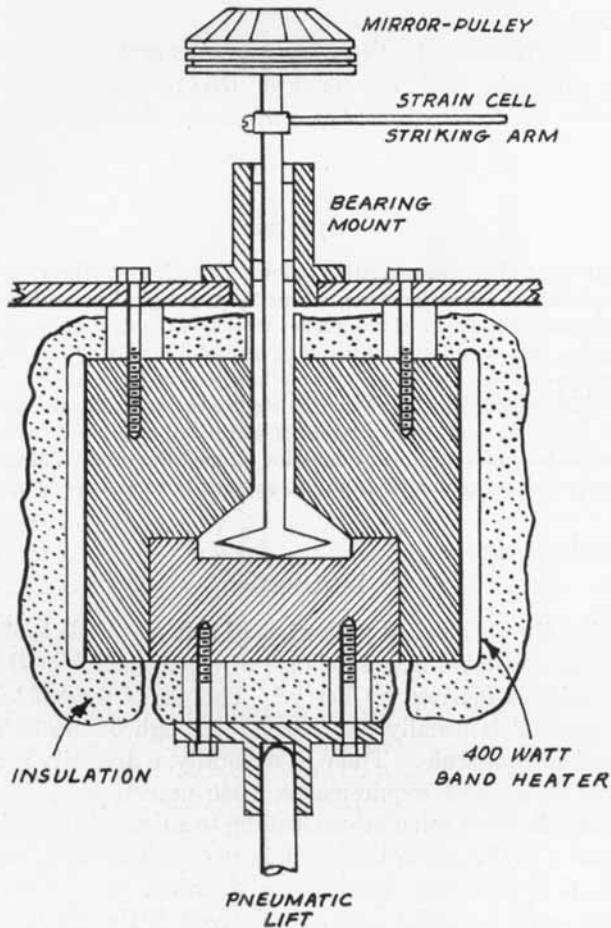


Fig. 1. Sectioned view of the cone-and-plate viscometer.

tribution toward longer times, which is especially useful when one is interested in the effects of molecular weight distribution. The long-time weighting can be clearly seen by examining the relaxation expressions resulting from use of the usual phenomenological models. For the stress $\sigma(t)$ at time t following cessation of flow at a steady shear rate $\dot{\gamma}_0$, one has

$$\frac{\sigma(t)}{\dot{\gamma}_0} \equiv \varphi(t) = \int_{-\infty}^{\infty} \tau H(\tau) e^{-t/\tau} d \ln \tau \quad (1)$$

Similarly, for the relaxation of stress $\sigma_s(t)$ following the sudden application of a strain γ_0 ,

$$\frac{\sigma_s(t)}{\gamma_0} = \int_{-\infty}^{\infty} H(\tau)e^{-t/\tau} d \ln \tau \quad (2)$$

Thus, eq. (1) has the relaxation distribution $H(\tau)$ weighted with an additional relaxation time τ . It is easy to obtain $\sigma_s(t)/\gamma_0$ by differentiation, if needed:

$$\frac{\sigma_s(t)}{\gamma_0} = - \frac{d}{dt} \left[\frac{\sigma(t)}{\dot{\gamma}_0} \right] \quad (3)$$

The second attractive feature of the steady-flow method is that it avoids the nonzero loading time inherent in the sudden-strain method. As will be discussed shortly, the initial portion of the steady-flow record involves only a change in slope, not a sudden change in stress level. While this record probably does not contain any more information, it does provide data in a somewhat less scattered form.

A third possible advantage of the steady-flow method lies in its experimental simplicity. For the measurements to be discussed in this paper, a more or less conventional cone and plate apparatus was used. Designed with advice from Dr. John P. Tordella, it is shown sectioned in Figure 1. The lower plate can be quickly dropped out by the pneumatic lift underneath, which shortens to a few minutes the time required to begin measurements on a disk-shaped sample. The rotatable upper shaft is held at a fixed vertical position by a pin passing through it and resting on the upper bearing. At the top of the shaft is a mirror-pulley combination. The multifaced aluminum mirror is used to reflect a parallel light beam into a Beckman Photo-Pen recorder so that creep and creep-recovery experiments may be performed on the same sample to be used for the relaxation measurements. The novelty of this apparatus lies mainly in the way by which the relaxing stress is measured. To do this, a rod is attached at right angles to the upper part of the shaft. After a condition of steady shearing has been achieved, this rod is allowed to strike a waiting strain cell. Stress buildup recorded by the strain cell is exactly equal to the stress decay suffered by the molten polymer. This scheme eliminates the usual torsion-rod mounts, and also allows the sample to be thermostatted accurately, since only one shaft protrudes from the instrument.

There is no need to calibrate the stress scale separately. Since the steady-state viscosity, η_0 , can be measured just prior to the beginning of relaxation, the ratio of stress to shear rate begins at η_0 and decays to zero. Hence the viscosity is the scale factor.

Empirical Representation

An empirical expression which has found some use for representing retarded elasticity data is the following:^{5,6}

$$J(t) = J_e [1 - \exp \{ -(t/\tau_1)^n \}] \quad (4)$$

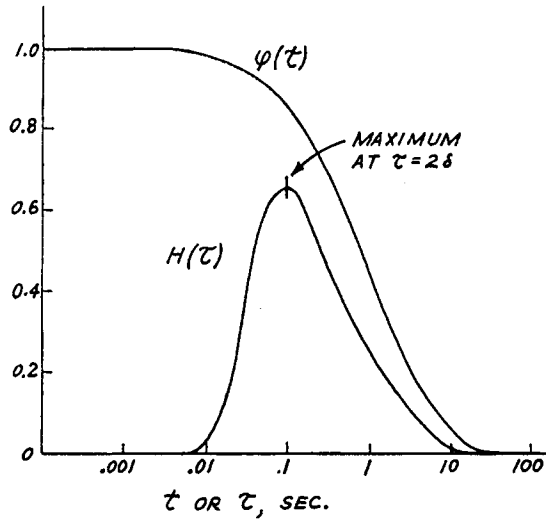


Fig. 2. Form of the relaxation curve and the distribution of relaxation times. Calculated from eqs. (5) and (6) of the text for $\eta_0 = 1$, $\tau_0 = 1$, $m = 0.5$, and $\delta = 0.05$.

where $J(t)$ is the recoverable elastic compliance at time t , J_e is the total time dependent compliance, and τ_1 and n are parameters. The exponent n is usually around 0.5.

For purposes of computation, extrapolation, and data storage it was considered desirable to attempt a similar empirical fit of steady-flow stress relaxation data. Even though there is a superficial resemblance between the relaxation and creep recovery curves, it was found to be necessary to add a small increment δ to the time before a good fit could be achieved. The resulting expression is:

$$\frac{(\sigma t)}{\dot{\gamma}_0} \equiv \varphi(t) = \eta(\dot{\gamma}_0) \exp \left\{ - \left[\left(\frac{t + \delta}{\tau_0} \right)^m - \left(\frac{\delta}{\tau_0} \right)^m \right] \right\} \quad (5)$$

where $\eta(\dot{\gamma}_0)$ is the steady-state viscosity at the shear rate $\dot{\gamma}_0$ prevailing before relaxation begins. The adjustable parameters are m , δ , and τ_0 . The necessity of adding an increment δ to the time may be explained qualitatively by consideration of the first derivative of the stress relaxation curve. As mentioned before, this slope at zero time is the negative of the so-called instantaneous modulus, and thus must be finite. However, without the δ the derivative of eq. (5) is infinite at zero time.

An example will probably show most clearly the effects of the parameters. In Figure 2 is shown a hypothetical relaxation curve, $\varphi(t)$, constructed from eq. (5) by using a unit viscosity and reasonable values of τ_0 , m , and δ . The distribution of relaxation times, $H(\tau)$, is obtained by inversion of eq. (1). When $m = 0.5$, $H(\tau)$ is obtainable directly as the inverse Laplace transform of $\varphi(t)$. This inversion yields

$$H(\tau) = \frac{\eta_0 \exp \{(\delta/\tau_0)^{0.5}\}}{2(\pi\tau_0\tau)^{0.5}} \exp \left\{ - \left(\frac{\delta}{\tau} + \frac{\tau}{4\tau_0} \right) \right\} \quad (6)$$

For $m \neq 0.5$ the inversion is more involved, requiring computer work, as recently discussed by Peticolas.⁷

The lower curve of Figure 2 is a plot of eq. (6). The value of δ affects the position of the maximum and the shape of the curve at short times. The average relaxation time τ_0 affects the curve shape at long times. A decrease in m causes an increased half width, though the exact relation is complicated.

For practically determining $H(\tau)$ from the experimental relaxation data, it is not difficult to apply the usual approximation methods involving first and higher derivatives,¹ since eq. (5) may be differentiated as much as necessary.

In order to fit eq. (5) by hand, it is best written in the form

$$\log \frac{\eta(\dot{\gamma}_0)}{\varphi(t)} = \frac{(t + \delta)^m}{2.3\tau_0^m} - \frac{\delta^m}{2.3\tau_0^m}$$

Log log $[\eta(\dot{\gamma}_0)/\varphi(t)]$ is plotted against log t and a line passed through the points at large values of t . The slope is taken as a trial m and the value of log log $[\eta(\dot{\gamma}_0)/\varphi(t)]$ at $t = 1$ taken as $1/2.3\tau_0^m$. The instantaneous modulus, G_0 , is determined from the initial slope of $\varphi(t)$ versus t . From G_0 a trial value of δ can be found:

$$G_0 = \eta(\dot{\gamma}_0)m\tau_0^{-m}\delta^{m-1} \quad (7)$$

When the first values for m , τ_0 , and δ have been obtained, then log $\{\log [\eta(\dot{\gamma}_0)/\varphi(t)] + (\delta^m/2.3\tau_0^m)\}$ is plotted against log $(t + \delta)$, and the process repeated until assumed and calculated parameters agree. Convergence is fast and for a number of different polymer melts $\varphi(t)$ can be fitted to within the error made in reading the chart record. Both $\eta(\dot{\gamma}_0)$ and τ_0 are rather directly dependent on the molecular weight of the polymer.

The δ will normally be small, typically ranging from 0.01 to 0.05. For narrow molecular weight distributions m will usually be in the vicinity of 0.5, down to perhaps 0.3 for broad distributions.

It is interesting that if a hypothetical relaxation curve is constructed with $m = 0.5$, and decomposed into a discrete distribution of relaxation times, these times will follow a Rouse-like⁸ sequence. Thus their values will be approximately proportional to members of the sequence 1, $1/4$, $1/9$, $1/16$, etc. A more rigorous connection between the empirical function and its model counterpart,

$$\varphi(t) = \sum_{i=1}^{\infty} \tau_i G_i \exp \{ -(t/\tau_i) \}$$

has not yet been worked out.

Example: Non-Newtonian Properties

A frequent problem associated with polymer melts and solutions is the specification of rheological properties such as the viscosity or elastic compliance at nonzero shear rates.

By using current viscoelastic theory and reasonable approximations it is possible to get a good idea of such non-Newtonian behavior without actually subjecting the material to extreme conditions. This is done by making direct use of the stress relaxation or creep-recovery curves. To obtain the necessary expressions, the molecular viscoelastic theory of Pao⁹ will be used. Accordingly, the viscosity at shear rate $\dot{\gamma}$ is written

$$\eta(\dot{\gamma}) = (1 + \gamma_R^2) \int_{-\infty}^{\infty} \frac{\tau H(\tau) d \ln \tau}{1 + \dot{\gamma}^2 \tau^2} \quad (8)$$

where γ_R represents the recoverable elastic strain, which need not be written out here. If eq. (8) is compared with eq. (1) for $\varphi(t)$, the integral portions are identical except for the step functions. If the approximation is made that, when $t = \dot{\gamma}^{-1}$,

$$(1 + \dot{\gamma}^2 \tau^2)^{-1} \cong 1 - \exp \{ -(t/\tau) \}$$

then one can integrate eq. (8) and obtain the approximate result:

$$\eta(\dot{\gamma}) \cong (1 + \gamma_R^2) [\eta(\dot{\gamma}_0) - \varphi(t = \dot{\gamma}^{-1})] \quad (9)$$

Assuming that $\eta(\dot{\gamma}_0)$ is the Newtonian viscosity and that γ_R is small, the following convenient form results:

$$\eta(\dot{\gamma}) \cong \eta_0 - \varphi(t = \dot{\gamma}^{-1}) \quad (10)$$

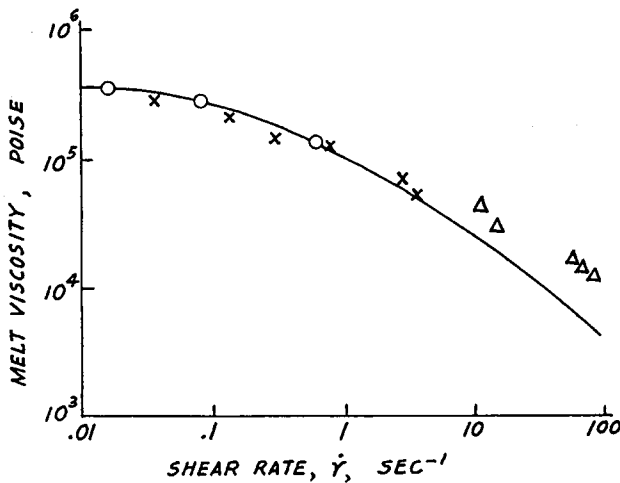


Fig. 3. Non-Newtonian viscosity for a polyethylene sample as obtained with (O): cone-and-plate viscometer; (X) a gas-pressured capillary rheometer; (Δ) a piston capillary rheometer. The line was calculated from stress-relaxation data by using eq. (10) of the text.

Use of this equation for quickly estimating high shear-rate viscosity from the stress relaxation curve requires only a replotting. The Newtonian viscosity, $\eta(\dot{\gamma}_0)$, minus the value of the relaxation curve at a time equal to the reciprocal shear rate is plotted against $\dot{\gamma} = t^{-1}$. Figure 3 shows such a plot for a low density polyethylene, melt index 2.1, at 150°C. The capillary data were obtained¹⁰ with the use of both gas and piston rheometers. The circles are measured viscosities obtained with the cone-and-plate viscometer, and the line is calculated from the empirical form for the stress-relaxation data [eq. (5)]. It is apparent from this use of the empirical function that it could also be used as a primary representation of viscosity-shear rate data itself.

It is appropriate to mention here an analogous approximation method to give the shear-rate dependence of the steady-state recoverable elastic compliance, $J_e(\dot{\gamma})$. The equation for this, as derived from Pao's theory⁹ is

$$J_e(\dot{\gamma}) = \int_{-\infty}^{\infty} \frac{L(\tau) d \ln \tau}{1 + \dot{\gamma}^2 \tau^2} \quad (11)$$

where $L(\tau)$ is the distribution of retardation times. By using the same level of approximation that gave eq. (9) for the viscosity, one finds for the elastic compliance:

$$J_e(\dot{\gamma}) \cong J(t = \dot{\gamma}^{-1}) \quad (12)$$

If eq. (4) is used to represent $J(t)$, one then has

$$J_e(\dot{\gamma}) \cong J_e(\dot{\gamma}_0) [1 - \exp \{ -(\dot{\gamma} \tau_1)^{-n} \}] \quad (13)$$

A concise way of displaying both the viscosity [eq. (9)] and elasticity

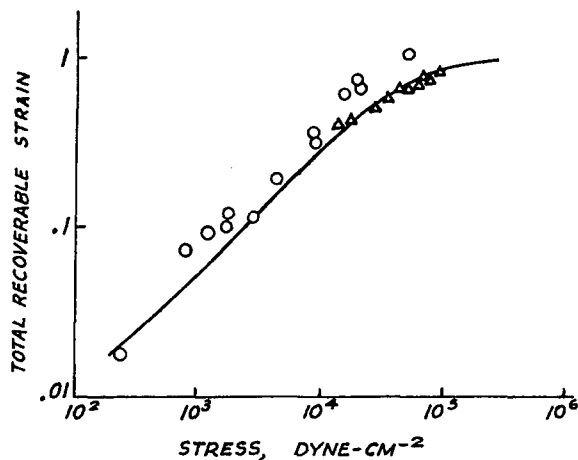


Fig. 4. Dependence of the total recoverable strain for a polyethylene sample upon applied shear stress, results obtained from (O) the cone-and-plate measurements; (Δ) extrudate swelling by a capillary with a length/diameter ratio of 195. The line was calculated from stress-relaxation and creep-recovery data by use of eq. (15) of the text.

[eq. (12)] results is afforded by the calculated total recoverable strain. This is equal to the stress times the total compliance:

$$\gamma(\dot{\gamma}) = \sigma[J_0 + J_e(\dot{\gamma})] \quad (14)$$

The total compliance is made up of the "instantaneous" part J_0 and the "time-dependent" part $J_e(\dot{\gamma})$. Writing the stress as the product of the shear rate and viscosity, and substituting G_0^{-1} for J_0 , one has

$$\gamma = \dot{\gamma}\eta[G_0^{-1} + J_e] \quad (15)$$

Figure 4 shows γ calculated using the experimental stress relaxation and creep recovery data from the same polyethylene as before. Extrapolation of the empirical expressions indicates that γ will rise to a maximum and ultimately return to a value of unity. This maximum can be seen experimentally, although the actual limiting strain probably cannot be predicted accurately by the empirical approach.

Example: Limiting Behavior at High Shear Rates

Using eqs. (5) and (10), the viscosity at a shear rate $\dot{\gamma}$ is approximately

$$\eta(\dot{\gamma}) = \eta(\dot{\gamma}_0) \left[1 - \exp - \left\{ \frac{(\delta + \dot{\gamma}^{-1})^m - \delta^m}{\tau_0^m} \right\} \right]$$

If this is expanded at high shear rates, the viscosity approaches the leading term, or

$$\eta(\dot{\gamma}) \rightarrow \frac{\eta(\dot{\gamma}_0)m\delta^{m-1}}{\dot{\gamma}\tau_0^m}$$

Referring to eq. (7) this can be rewritten as

$$\eta(\dot{\gamma}) \rightarrow G_0/\dot{\gamma} \quad (16)$$

Such an expression is unsatisfactory as it stands since a stress is being equated to a modulus. In other words, if we designate the proper form of eq. (16) as

$$\eta(\dot{\gamma}) \rightarrow \gamma_m G_0/\dot{\gamma} \quad (17)$$

then eq. (16) requires γ_m , a strain term, to be unity. Retaining the form of eq. (17) implies a limiting stress equal to $\gamma_m G_0$.

At fairly high shear rates there is a phenomenon in capillary extrusion known as melt fracture.¹¹ There is experimentally a critical stress at which this fracture occurs and it is tempting to associate with it the limiting stress as indicated by the viscosity extrapolation. Figure 5 shows a plot of the critical shear stress against the instantaneous modulus for several polymers.¹² The correlation is reasonably good, and leads to a value of 5 for the strain at fracture. This agrees with the result obtained experimentally by Spencer.¹³ Such a correlation encourages a possible explanation of melt fracture which does not involve concepts of inlet instabilities or other geometric causes, as have been proposed from time to time.

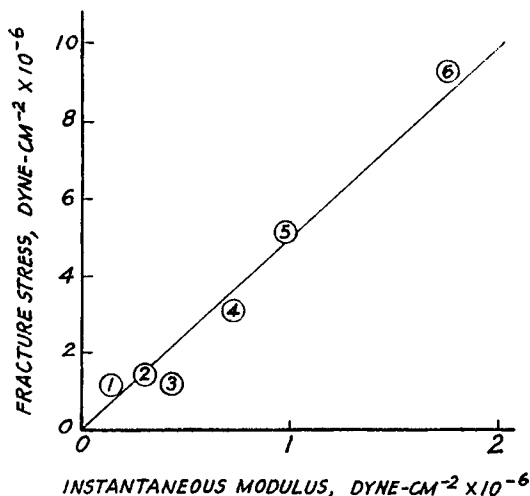


Fig. 5. Comparison of fracture stress using 3.65 length/diameter ratio capillary with instantaneous modulus for various polymers: (1) polyethylene at 150°C., M.I. 2.1, density 0.917; (2) polyethylene at 150°C., M.I. 2.0, density 0.923; (3) polyethylene at 150°C., M.I. 2.0, density 0.914; (4) linear polyethylene at 150°C., M.I. 0.50, density 0.958; (5) poly(methyl methacrylate) at 200°C.; (6) high polymer of formaldehyde (polyoxymethylene) at 200°C.

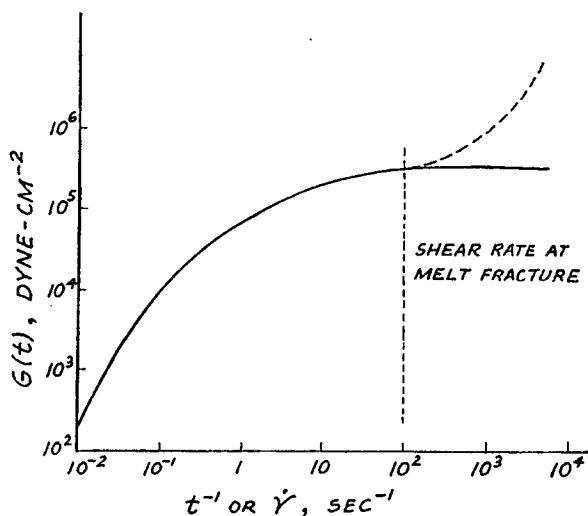


Fig. 6. Dependence of shear modulus on shear rate for a polyethylene sample. Calculated from stress relaxation data by use of eq. (3) of the text.

Figure 6 shows the relaxation modulus, $\sigma_s(t)/\gamma_0$, plotted against reciprocal time or, nearly, shear rate, for the same polyethylene as before. This was calculated by using eqs. (3) and (5), and can therefore show only a plateau at short times, though in this range there should begin another rise through

the glass transition. The height of the plateau is the instantaneous modulus.

Since coordinated center-of-mass motion is becoming impossible as the glass transition is reached, one may say that the probable cause of melt fracture is the flow of clusters involving more than one molecule. This is, in fact, a rupture or yield and thus requires the large shear strain of some five units. The experimental shear rate at which melt fracture occurs is shown as a vertical dashed line. It is assumed that the rise through the glass transition would begin shortly thereafter, as shown by the dashed curve. For more accurate representation at these short times, some improvement of the empirical function would be needed, though it is not indicated by the requirement of fitting the experimental data.

Example: True Newtonian Viscosity

When viscosities are measured with mechanical apparatus, there must necessarily be some flow of the sample. For high molecular weight polymers this nonzero shear rate, even though quite small, may already be large enough that the material is non-Newtonian.

By assuming correctness of the hydrodynamic theory at low shear-rates, it is often possible to calculate a true zero shear-rate viscosity. At a small shear rate $\dot{\gamma}_0$ the viscosity is, by eq. (8),

$$\eta(\dot{\gamma}_0) = \int_{-\infty}^{\infty} \frac{\tau H^*(\tau) d \ln \tau}{1 + \dot{\gamma}_0^2 \tau^2} \quad (18)$$

where $H^*(\tau)$ represents the relaxation distribution which would be obtained under true zero shear-rate conditions. From stress relaxation measurements made after steady flow at a shear rate $\dot{\gamma}_0$, one would calculate an experimental $H(\tau)$, so that

$$\eta(\dot{\gamma}_0) = \int_{-\infty}^{\infty} \tau H(\tau) d \ln \tau \quad (19)$$

Thus, equating the integrands of eqs. (18) and (19), one has

$$\tau H^*(\tau) = \tau H(\tau) [1 + \dot{\gamma}_0^2 \tau^2] \quad (20)$$

At a hypothetical zero shear rate the true Newtonian viscosity would be

$$\eta_0 = \int_{-\infty}^{\infty} \tau H^*(\tau) d \ln \tau \quad (21)$$

Putting eq. (20) into this expression one obtains

$$\eta_0 = \eta(\dot{\gamma}_0) + \dot{\gamma}_0^2 \int_{-\infty}^{\infty} \tau^3 H(\tau) d \ln \tau \quad (22)$$

Equation (22) contains an additive correction term involving a fairly high moment of the relaxation distribution. It is possible to derive a general expression for the evaluation of any moment of the relaxation distribution in terms of experimental quantities. (See Appendix.) It is

$$\int_{-\infty}^{\infty} \tau^{2+\nu-n} H(\tau) d \ln \tau = \frac{(-1)^{n+2}}{\nu!} \int_0^{\infty} t^\nu \frac{d^n \varphi(t)}{dt^n} dt \quad (23)$$

Now, by choosing $n = 1$ and $\nu = 0$, eq. (22) is reduced by eq. (23) to

$$\eta_0 = \eta(\dot{\gamma}_0) + \dot{\gamma}_0^2 \int_0^\infty t \varphi(t) dt \quad (24)$$

If the empirical function, eq. (5), is now used, and very small terms neglected, eq. (24) may be integrated to the form

$$\eta_0 = \eta(\dot{\gamma}_0) \left[1 + \frac{\dot{\gamma}_0^2 \tau_0^2}{2} \left(\frac{2}{m} \right)! \exp \left\{ \left(\frac{\delta}{\tau_0} \right)^m \right\} \right] \quad (25)$$

In Table I the magnitude of this correction is shown for a none-too-drastring example—a linear polyethylene with $\bar{M}_w = 1.2 \times 10^5$, measured at 173°C.

TABLE I
Calculated True Newtonian Viscosity

$\dot{\gamma}_0$, sec. ⁻¹	$\eta(\dot{\gamma}_0)$, poise $\times 10^{-5}$	η_0 (calc.), poise $\times 10^{-5}$
0.046	2.60	2.82
0.131	2.29	2.76

Appendix

Derivation of eq. (23) is as follows.

The integral I is defined as

$$I = \int_0^\infty t^\nu (d^n \varphi / dt^n) dt$$

where

$$\varphi = \int_{-\infty}^\infty \tau H(\tau) \exp \{ -(t/\tau) \} d \ln \tau$$

Taking the n th derivative,

$$\frac{d^n \varphi}{dt^n} = (-1)^{n+2} \int_{-\infty}^\infty \tau^{1-n} H(\tau) \exp \{ -(t/\tau) \} d \ln \tau$$

Then

$$I = \int_0^\infty t^\nu [(-1)^{n+2} \int_{-\infty}^\infty \tau^{1-n} H(\tau) \exp \{ -(t/\tau) \} d \ln \tau] dt$$

or

$$I = (-1)^{n+2} \int_{-\infty}^\infty \tau^{1-n} H(\tau) [\int_0^\infty t^\nu e^{-t/\tau} dt] d \ln \tau$$

Now, since

$$\int_0^\infty t^\nu e^{-t/\tau} dt = \nu! \tau^{\nu+1}$$

one has then eq. (23):

$$\int_{-\infty}^\infty \tau^{2+\nu-n} H(\tau) d \ln \tau = \frac{(-1)^{n+2}}{\nu!} \int_0^\infty t^\nu \frac{d^n \varphi(t)}{dt^n} dt$$

Incidentally, this result is useful for experimentally determining various moments of the molecular weight distribution as previously derived.¹⁴ In that reference the following equation was obtained to relate the α th moment of the weight distribution to the mechanical model:

$$\int_0^{\infty} M^{\alpha} W(M) dM = \beta \int_{-\infty}^{\infty} H(\tau) \tau^{(\alpha+1)/2} d \ln \tau$$

where β is a constant for the sample, involving \bar{M}_w , the sample viscosity, and temperature. By using eq. (23) this expression becomes, for $n = 0$,

$$\int_0^{\infty} M^{\alpha} W(M) dM = \frac{\beta(-1)^{n+2}}{[(\alpha - 3)/2]!} \int_0^{\infty} t^{(\alpha-3)/2} \varphi(t) dt$$

In this form it is convenient for numerical evaluation.

Reference to a company or product name does not imply approval or recommendation of the product by the U. S. Department of Agriculture to the exclusion of others that may be suitable.

References

1. Ferry, J. D., *Viscoelastic Properties of Polymers*, Wiley, New York, 1961.
2. Schremp, F. W., J. D. Ferry, and W. W. Evans, *J. Appl. Phys.*, **22**, 711 (1951).
3. Watkins, J. M., *J. App. Phys.*, **27**, 419 (1956).
4. Watkins, J. M., R. D. Spangler, and E. C. McKannan, *J. Appl. Phys.*, **27**, 685 (1956).
5. Kargin, V. A., and G. L. Slonimskii, *Acta Physicochim. (U.S.S.R.)*, **12**, 931 (1940).
6. Leaderman, H., R. G. Smith, and R. W. Jones, *J. Polymer Sci.*, **14**, 47 (1954).
7. Peticolas, W. L., presented at October 29-31 1962 Meeting of the Society of Rheology, Baltimore.
8. Rouse, P. E., Jr., *J. Chem. Phys.*, **21**, 1272 (1953).
9. Pao, Y. H., *J. Polymer Sci.*, **61**, 413 (1962).
10. Tordella, J. P., private communication.
11. Tordella, J. P., *Rheol. Acta*, **1**, 216 (1958).
12. Tordella, J. P., *J. Appl. Polymer Sci.*, **7**, 215 (1963).
13. Spencer, R. S., *J. Polymer Sci.*, **5**, 591 (1950).
14. Menefee, E., and W. L. Peticolas, *J. Chem. Phys.*, **35**, 946 (1961).

Résumé

La mesure de la tension de relaxation consécutive à un cisaillement stationnaire particulièrement utile dans la zone de relaxation terminale où les propriétés rhéologiques dépendant du poids moléculaire. Cette publication contient une description de la méthode telle qu'elle est appliquée aux polymères fondus et une fonction empirique qui s'est avérée utile pour l'adaptation des résultats. On donne trois exemples qui démontrent quelques applications simples et directes. En premier lieu, la diminution de viscosité en augmentant la vitesse de cisaillement peut être estimée en reportant graphiquement les résultats expérimentaux. En second lieu, on montre que l'extrapolation des viscosités calculées pour des vitesses très élevées de cisaillement conduit à une explication possible des ruptures à la fusion. En troisième lieu, on peut estimer la viscosité newtonienne vraie au départ de mesures conduites à une vitesse de cisaillement nulle.

Zusammenfassung

Die Messung der einer stationären Scherung folgenden Spannungsrelaxation ist bei der Endrelaxation, bei welcher die rheologischen Eigenschaften vom Molekulargewicht abhängig sind, von besonderem Nutzen. Die vorliegende Arbeit gibt eine Beschreibung der auf geschmolzene Polymere angewandten Methode und eine zur Einordnung der Daten gut brauchbare empirische Funktion. An drei Beispielen werden einige direkte und einfache Anwendungsmöglichkeiten gezeigt. Erstens kann durch eine einfache Neuauftragung der experimentellen Daten die Viskositätsabnahme mit steigender Scherungsgeschwindigkeit bestimmt werden. Zweitens führt die Extrapolation der berechneten Viskositäten auf sehr hohe Scherungsgeschwindigkeit zu einer möglichen Erklärung für den Bruchvorgang in der Schmelze. Drittens kann durch Messungen bei einer von Null verschiedenen Scherungsgeschwindigkeit die wahre Newtonsche Viskosität bestimmt werden.

Received March 25, 1963